What is best strategy for water soluble fluorescence dyes? – A case study using long fluorescence lifetime DAOTA dyes

Niels Bisballe[a] and Bo W. Laursen*[a]

Address:

[a] Nano-Science Center & Department of Chemistry, University of Copenhagen, Universitetsparken 5, DK-2100, Copenhagen Ø, Denmark.

* Corresponding author e-mail:

bwl@nano.ku.dk

Abstract

The applications of organic fluorophores in biological sciences rely heavily on their properties in aqueous solution. The lipophilic nature of virtually all such chromophores provides several challenges to adapt them to biologically relevant conditions. In this work we investigate three different strategies for achieving water-solubility of the diazaoxatriangulenium ($DAOTA^+$) chromophore: hydrophilic counter ions, aromatic sulfonation of the chromophore core, and attachment of cationic or zwitterionic side chains. The long fluorescence lifetime (FLT, $\tau_f \approx 20$ ns) of $DAOTA^+$ makes it a sensitive probe for changes in the rate of non-radiative deactivation and for aggregation leading to multi exponential decay profiles. Direct sulfonation of the chromophore, as applied in several Alexa dyes, does indeed increase solubility drastically, but at the cost of greatly reduced quantum yields (QY) due to enhanced non-radiative deactivation processes. The introduction of either cationic (4) or zwitterionic side chains (5), however, brings the FLT ($\tau_f = 18$ ns) and QY ($\varphi_f = 0.56$) of the dye to the same level as the parent chromophore in acetonitrile. For these derivatives time-resolved fluorescence spectroscopy also reveals a high resistance to aggregation and non-specific binding in a high loading of bovine serum albumin (BSA). The results clearly show that addition of charged flexible side chains is preferable to direct sulfonation of the chromophore core.

Introduction

Molecular behavior of a solute in a given solvent is a critical property in several chemical sciences, ranging from the distribution of drugs in the human body to the self-assembly of nanostructures.[1, 2] This is indeed also the case in the field of bio-imaging and for assays relying on fluorescent dyes, where enhanced water solubility of dyes leads to improved signal to background ratios and elimination of artifacts.[3-5]

Organic chromophores in general consist of extended π-conjugated systems responsible for absorption and emission of ultra-violet (UV) to near-infrared (NIR) electromagnetic radiation. This inherently introduces a hydrophobic structural element to the fluorescent molecule, favoring dissolution in organic solvents, while inducing aggregation due to poor solvation in aqueous environments.[6, 7] In bio-imaging the latter is seldom desirable, but notable exceptions include the probing of membranes and staining lipophilic compartments.[8, 9] Dye aggregation may lead to unwanted changes in absorption and emission spectra, reduced fluorescence intensity and lifetime.[10-13] But even when aggregates are avoided e.g. by high dilution, moderate water-solubility may still lead to problems arising from hydrophobic interactions with other amphiphilic solutes such as biomacromolecules. This may lead to nonspecific binding and can in turn also alter optical properties.[14-17] Thus, for general application of fluorescence dyes, high water-solubility is a key feature since it is expected to reduce both dye-dye interactions (aggregation and self-quenching) as well as nonspecific interactions with biomolecules.

A testament to the importance of good solvation of fluorescent probes in aqueous media is the pioneering work of Haugland leading to the highly successful commercial Alexa Fluor® dyes (Thermo Fisher).[18, 19] The Alexa Fluor® dyes are traditional organic chromophores, mainly xanthenes and cyanines, modified with anionic sulfonate groups to drastically increase their water solubility and thus performance in bioimaging. The same strategy has since been employed for several other chromophore types and by other commercial brands.

While many different chromophore modifications have been applied for increasing water-solubility, including anionic sulfonates and phosphonates, zwitterionic sulfobetaines and neutral PEG chains, there is presently no general consensus about the preferred or optimal modifications of fluorescence dyes to increase water-solubility and minimize artefacts in bio-imaging. Rhodamine and borondipyrromethene (BODIPY) chromophores are popular in bioimaging and

enhancing their water-solubility is a desirable improvement. A key feature of these dyes is their high brightness ($\varepsilon \cdot \varphi_f$). They also feature moderate fluorescence lifetimes (FLTs) in the range of 3-5 ns and have seen application in time resolved fluorescence spectroscopy.[20-22] Inspired by the Alexa Fluor® dyes, Kolmakov *et al.* (2010) have synthesized a red emitting, water-soluble rhodamine dye by allylic sulfonation.[23] They have successfully demonstrated the use of the dye in advanced super-resolution fluorescence imaging techniques. Since, Kolmakov *et al.* (2012) have also assessed the solubilizing effects of phosphonate and hydroxyl groups in the same position.[24]

Investigations into solubilizing the BODIPY chromophore are more varied. Early examples carry sulfonate groups directly on the chromophore.[25, 26] Later investigations have focused on introducing water solubility through functionalized side chains to keep the electron distribution of the chromophore intact. The solubilizing groups are typically comprised of sulfonates, phosphonates and sulfobetaines.[27-29]

Another successful approach to water solubility has been post-synthetic functionalization of dyes with a sulfonated peptide linker. The linker can be introduced through well-known couplings like amidation and the *click*-reaction, which many commercially available dyes are already set up for.[30-32] This strategy, however, seems to work best for dyes that already contain hydrophilic elements. The peptide linker may feature further functional groups suitable to generate bioconjugates.[33]

We have in recent years been working with synthesis and applications of various aza-/oxa-triangulenium dyes (Chart 1), in particular the $ADOTA^+$ and $DAOTA^+$ derivatives. These fluorophores display especially long intrinsic FLT in combination with good quantum yield (QY), making them uniquely suited for time-gated imaging[34], fluorescence lifetime imaging microscopy (FLIM)[35, 36] and fluorescence polarization assays[37, 38]. The long FLT arises from the combination of moderate radiative rate (k_f) and very low rates of non-radiative deactivation (k_{nr}).[39] The major challenge in designing and modifying long FLT dyes is to keep the rate of non-radiative deactivation very low. which is achieved through exceptional structural rigidity.

In this work we investigate design strategies to obtain highly water soluble triangulenium dyes. Firstly, such modifications have not been made before and would greatly increase the scope of these unique long FLT dyes. Secondly, the long FLT of these dyes provide a highly sensitive test case to compare various strategies for enhancing water solubility. This sensitivity arises from the intrinsically lower rate of fluorescence, which ensures that any additional non-radiative

contributions to deactivation of the excited state will have a much greater impact than in standard fluorophore systems with a shorter lifetime. We will also use fluorescence lifetime measurements as a convenient tool to probe the degree of aggregation and/or association with bio molecules as any of such events will lead to inhomogeneity in the population of dyes and thus deviations from simple single exponential fluorescence decay rates.

The $DAOTA^+$ chromophore (Chart 1) was chosen as the starting point for this study. It features a long FLT ($\tau_f > 20$ ns in MeCN and DCM) and a high quantum yield ($\varphi_f = 0.58$ in MeCN, 0.80 in DCM).[39]

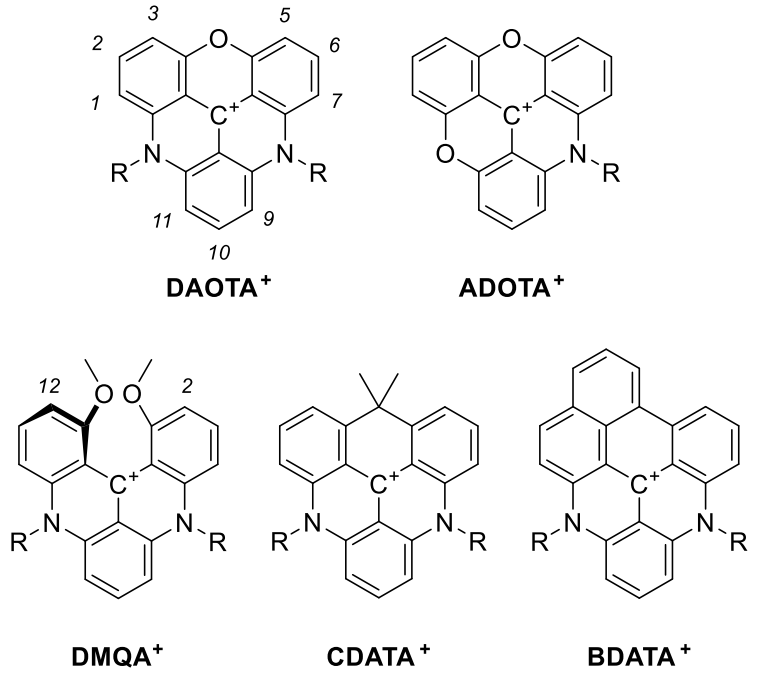

Chart 1. Structures of diazaoxatriangulenium ($DAOTA^+$), azadioxatriangulenium ($ADOTA^+$), dimethoxyquinacridinium ($DMQA^+$), carbon-bridged diazatriangulenium ($CDATA^+$) and benzo-fused diazatriangulenium ($BDATA^+$).

The $DAOTA^+$ chromophore is promising due to high photo stability[40, 41] and resistance to quenching from amino acids.[42] However, it suffers from low water solubility, which reduces its brightness and FLT in aqueous solutions. The chromophore is closely structurally related to other reported cationic triangulenium fluorophores such as: $ADOTA^+$ [43], $DMQA^+$ [44], $CDATA^+$ [45] and

BDATA$^+$ [46] dyes (Chart 1), but also to other much studied cationic dyes including helicenes[47, 48], acridines[49, 50] and rhodamines[51, 52]. Thus, we expect the here derived guidelines to be generally applicable to a large range of cationic fluorescent dyes.

Results and discussion

Strategies for chromophore modifications and synthesis

With a series of six new DAOTA$^+$ dyes (Chart 2) we will evaluate various strategies for increased water-solubility: 1) Introduction of hydrophilic counter ions. 2) Direct sulfonation of the chromophore system. 3) Addition of charged side chains. Traditionally, triangulenium dyes have been synthesized with the highly lipophilic tetrafluoroborate (BF_4^-) and hexafluorophosphate (PF_6^-) anions.

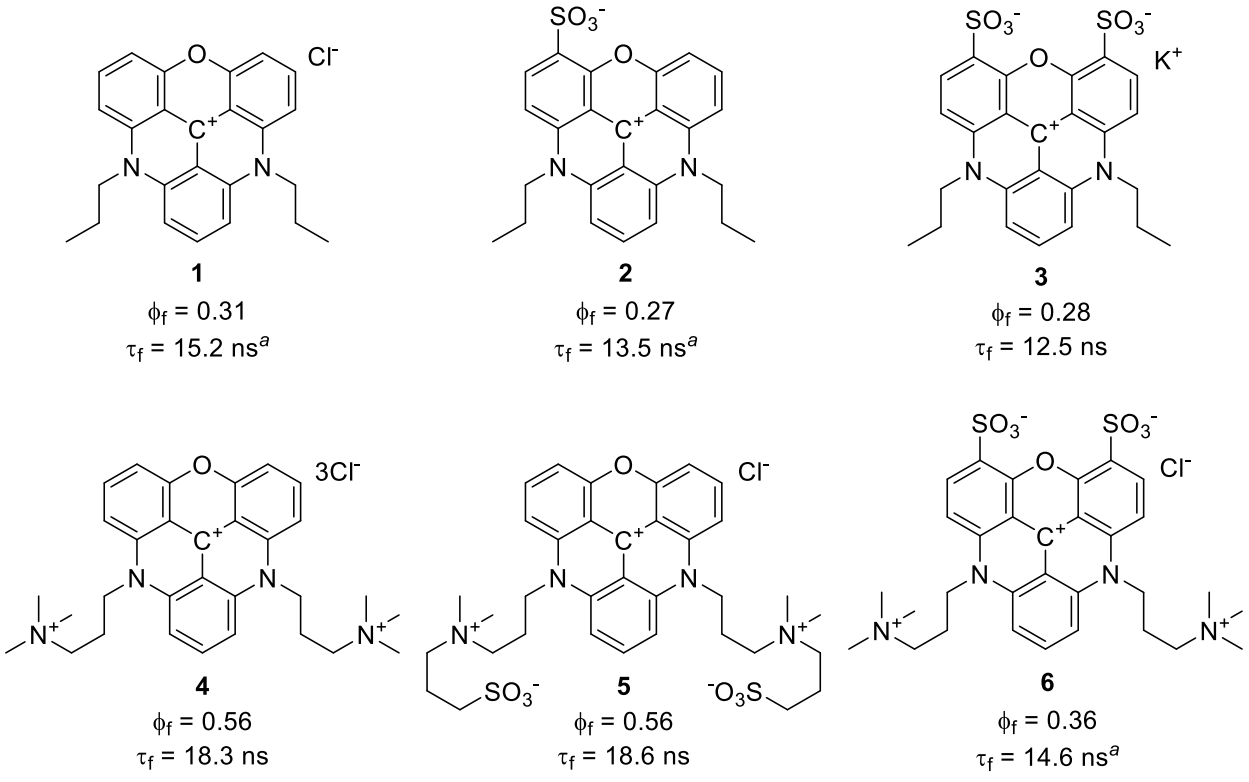

Chart 2. Structures of the six water-soluble DAOTA$^+$ dyes **1**-**6**, along with their QYs (φ_f) and FLTs (τ_f) in pure water. [a] Only the FLT corresponding to the freely solvated dye of a bi-exponential decay is shown (see Table 2 for details).

This strategy was developed with facile synthetic workup in mind, exploiting the lack of dissociation of these salts in aqueous media.[53] To obtain water-soluble derivatives, the anion of Pr_2DAOTA^+ was exchanged for the hydrophilic and biologically prevalent chloride ion. This was conveniently achieved using an anion exchange resin. This simple modification resulted in the highly water-soluble (>10 mM) dye, **1** (Chart 2), from the practically insoluble BF_4^- salt in quantitative yield (Scheme S1).

As mentioned in the introduction direct sulfonation of the chromophore core has been successfully applied in several cases, including Alexa 488 and Alexa 532 to name a few,[16] as well as the aforementioned BODIPY dyes. Functionalization directly on the $DAOTA^+$ chromophore can roughly be broken down to occur in three different regions: the positions neighboring the *O*-bridge (positions 3 and 5, Chart 1), positions neighboring the *N*-bridges (positions 1, 7, 9 and 11), and positions *para* to the carbenium center (positions 2, 6 and 10). Delgado *et al.* (2018) have shown large effects of simple functional groups attached directly to the 9-position of $DAOTA^+$ *via* electrophilic aromatic substitution, with a clear connection between electron density (donating/withdrawing groups) and spectral properties.[54] This is in line with observations from the $DAOTA^+$ precursor, $DMQA^+$.[55] We suspect that substitution neighboring the *O*-bridge is preferable to positions neighboring the *N*-bridge, since steric interference with the side-chain in the latter case is expected to reduce planarity. Despite EWGs on the 6-position enhancing fluorescence of the helical $DMQA^+$ [55], in planar systems functionalization next to *N*-bridges has a negative impact on fluorescence properties (QY and FLT) as seen for $DAOTA^+$, and in our previous observations with chlorination of triazatriangulenium salts. [54, 56]

Selective core sulfonation on the 3- and 5-positions of $DAOTA^+$ was achieved by overnight reaction in concentrated sulfuric acid (Scheme S1). A trace amount of the mono-sulfonated product (**2**) could also be obtained in this way, with the primary product containing sulfonates in both positions (**3**, 88 % yield). The mono-sulfonated product is likely to be a result of desulfonation during aqueous workup. Both products are soluble in water. The selectivity for the 3- and 5-positions is result of the strongly acidic conditions which favors electrophilic substitution in positions most remote to the nitrogen bridges, as reported by Duwald *et al.* (2017) for the $DMQA^+$ system (Chart 1).[57]

Modifying the dye with solvating groups on the side chains is expected to have little influence on the photophysics. We have several examples of $DAOTA^+$ modified in these positions, where the emissive properties intrinsic to the chromophore remain largely intact.[35, 39, 42] The side-chain modified dyes were synthesized via the traditional pathway for triangulenium dyes where side chains are introduced by substitution with primary amines during formation of the nitrogen bridges in the ring system.[53] By this classical pathway a $DAOTA^+$ dye carrying two 3-dimethylaminopropyl side chains (**9**, Scheme S2) was obtained as a key intermediate. Methylation of **9** with iodomethane gave tri-cationic **4** after anion exchange. Zwitterionic side chains were conveniently obtained by alkylation of **9** with 1,3-propanesultone, as previously reported for the CalFluor chromophores[58], to give **5** after anion exchange.

Finally, we were interested in combining the above strategies. By sulfonating the PF_6^- salt of **4** under conditions similar to the synthesis of **3**, **6** was obtained after anion exchange (Scheme S2). Full experimental details and characterizations of all new compounds are given in Supporting Information.

Photophysical properties of water-soluble triangulenium dyes

With this diverse set of water-soluble triangulenium dyes (**1**-**6**) in hand, we first investigated the effects of the modifications on the spectral features. As expected for the simple anion exchange absorption and emission are nearly identical for **1** and Pr_2DAOTA^+ (Table 1). Absorption spectra of **2** and **3**, containing one and two sulfonic acid groups respectively, were surprisingly similar. These modifications introduce a redshift in both absorption ($S_0 \rightarrow S_1$) and emission maxima compared to those of **1** (Table 1, Figure 1). The ($S_0 \rightarrow S_2$) absorption maximum on the other hand is blueshifted. The ionic side chains of **4** and **5** resulted in a blueshift shift in both ($S_0 \rightarrow S_1$) absorption and emission maxima. The ($S_0 \rightarrow S_1$) absorption band of both **4** and **5** are narrower than observed for **1** and Pr_2DAOTA^+ (Figure 1). For comparison, the absorption spectrum of **5** is similar in width and shape to the parent chromophore, Pr_2DAOTA^+ in MeCN, while **1** has less pronounced features (Figure S13).

Table 1 Steady state absorption and emission values for **1-6** (Chart 1) in water and Pr_2DAOTA^+ in acetonitrile for comparison. Full absorption and emission spectra as well as excitation specta for **1-6** can be found in the ESI (Figures S1-S6).

	Solvent	**λ_{max} (abs) [nm] $S_0 \rightarrow S_1$**	**λ_{max} (abs) [nm] $S_0 \rightarrow S_2$**	**λ_{max} (em) [nm] $S_1 \rightarrow S_0$**	**Stokes shift [cm^{-1}]**	**φ_f[a]**
$Pr_2DAOTA^{+\,b,\,c}$	MeCN	557	449	590	1004	0.58
1	H_2O	558	449	587	885	0.31
2	H_2O	564	440	594	895	0.27
3	H_2O	565	435	594	864	0.28
4	H_2O	549	448	576	854	0.56
5	H_2O	548	449	576	887	0.56
6	H_2O	558	439	584	798	0.36

a Quantum yields are determined relative to Rhodamine 6G in ethanol (φf = 0.95). Details on their calculation can be found in the ESI. b Data for Pr2DAOTA+ taken from Bogh et al. (2017)39. c Full absorption spectrum can be found in Figure S13.

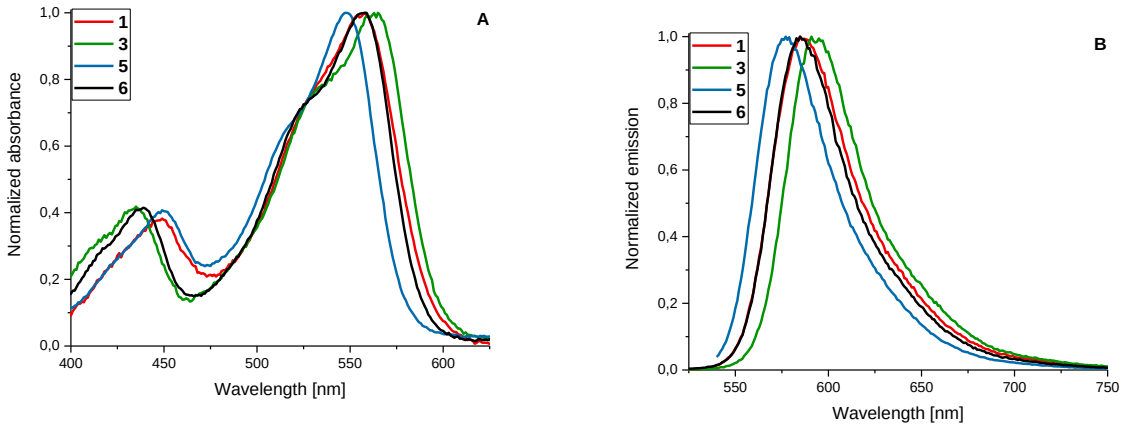

Figure 1. (A) Normalized overlay of absorption spectra of the DAOTA+ chromophore without modifications (**1**), with a sulfonated core (**3**, similar to **2**), with ionic side chains (**5**, similar to **4**) and both of the latter modifications combined (**6**). (B) Normalized overlay of emission spectra, analogous to A.

A narrower absorption band is an indication of a more homogeneous solvation, validating the strategy of placing the functional groups on the side chains. Combining the approaches of sulfonating directly on the chromophore and having quaternary ammonium groups on the side chains (**6**) results in spectra clearly relatable to each individual modification: the ($S_0 \rightarrow S_1$) absorption redshift of the sulfonic acid groups, as observed for **2** and **3**, and blue shift of the

charged side chains, as observed for **4** and **5**, counteract. The resulting absorption maximum is similar to that of **1**, which contains neither modification. The blue shift of the ($S_0 \rightarrow S_2$) absorption observed for **2** and **3**, and attributed to the sulfonic acid groups, persists in **6** as this transition is unaffected by the ammonium side chains.

The spectral shifts can be explained by the electronic effects of the modifications on the electronic transitions (Figure 2). The ($S_0 \rightarrow S_1$) transition is dominated by the *N*-bridges donating electron density to the formal cation center. The positively charged ammonium groups of the side chains in **4** and **5** poses an electrostatic influence on the *N*-bridges impeding this process, leading to a blueshift of the transition. Similarly, the sulfonates neighboring the *O*-bridge reduce its donating capabilities in the ($S_0 \rightarrow S_2$) transition. The ($S_0 \rightarrow S_1$) redshift from the sulfonates is surprising considering its position,[59] and we speculate that it might be a secondary effect of the S_2 blueshift reducing the mixing of S_1 and S_2 and thus increasing their separation.

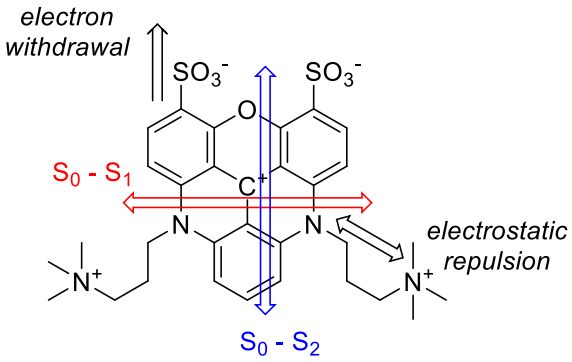

Figure 2. Substituent effects on the electronic transition dipoles for the first (red) and second (blue) excited state illustrated for **6**.[43] The electron donating capabilities of the heteroatom bridges is reduced in both cases, leading to more energetic transitions.

Despite the similar spectral properties of **1** and Pr_2DAOTA^+, the QY (Table 1) is almost halved for the former in aqueous solution. This can in part be attributed to poorer solvation of the cation in water compared to acetonitrile. A broadening of both absorption and emission bands were observed with increased dye concentration when measuring the QY, suggesting aggregation (Figures S23-S24).

However, an intrinsic quenching of fluorescence observed for dyes dissolved in water must also be considered to be a significant contribution. The extent of this effect can be determined by comparing the fluorescence in water and deuterium oxide and is discussed later in this work.

Direct sulfonation of the π-system lead to a decreased QY. When comparing the absorption and emission spectra from the QY titration of **2**, a slight broadening of the bands is seen with increased concentration which could indicate aggregation (Figures S26-S27). No broadening is observed for the double sulfonated **3** (Figures S29-S30), but the QY was still as low as **1**.

We were pleased to find that the QYs of **4** and **5** in water (Table 1) are comparable to that of Pr_2DAOTA^+ in MeCN. Introducing solubilizing groups on the side chains of $DAOTA^+$ promises to be a viable strategy in translating the desired photophysical properties to aqueous solution. The QY of **6** lies between the values resulting from the individual modifications (**3** and **4** respectively). This confirms that introducing the sulfonic acid groups has a negative impact on the QY.

Time resolved fluorescence spectroscopy in water

In order to explain the differences in QY of the synthesized dyes and to develop insight into the dyes' molecular behavior in aqueous solution, we turned to time-resolved fluorescence spectroscopy. Measuring the FLT and looking at the decay profiles allows us to distinguish well-solvated dyes displaying a mono-exponential fluorescence decay due to the homogeneity of the sample from inhomogeneous samples containing subpopulations of aggregated dyes and thus displaying multi exponential decay profiles. We found that in pure water only the dyes **3**-**5** display mono-exponential fluorescence decays (Table 2) and can be considered fully and homogeneously solvated.

The bi-exponential decay of **1** in water indicates poor solvation and the formation of aggregates, which show a longer lifetime component. The quantum yield of **1** is almost half (Table 1) compared to the best dyes (**4** and **5**) while the dominant FLT component only is reduced by 20%. This means that the observed aggregates must have very low quantum yields and/or non-emissive aggregates are also present.

Table 2. Comparison of fluorescence lifetimes of **1**-**6** (Chart 1) in water, PBS and PBS with the addition of BSA (600 µM). Full decay profiles can be found in the ESI (Figures S14-S19).

	H_2O			PBS			PBS + BSA			
	τ_{f1} [ns]	τ_{f2} [ns][a]	τ_{avg} [ns][b]	τ_{f1} [ns]	τ_{f2} [ns][a]	τ_{avg} [ns][b]	τ_{f1} [ns]	τ_{f2} [ns][a]	τ_{f3} [ns][a, c]	τ_{avg} [ns][b]
1	15.2	22.6 (19 %)	16.6	14.9	21.6 (26 %)	16.6	10.5	18.3 (60 %)	1.3 (1 %)	15.0
2	13.5	24.1 (12 %)	14.8	11.7	16.5 (54 %)	14.3	12.3	23.2 (51 %)	1.6 (2 %)	17.7
3	12.5	-	-	11.5	20.2 (7 %)	12.1	11.9	25.0 (59 %)	1.8 (1 %)	19.5
4	18.3	-	-	18.1	-	-	18.6	-	7.7 (3 %)	18.2
5	18.6	-	-	18.3	-	-	18.5	-	6.3 (2 %)	18.3
6	14.6	20.5 (7 %)	15.0	14.2	-	-	14.1	-	2.4 (1 %)	14.1

[a] Secondary fluorescence lifetime components and their weighted intensities in parenthesis. [b] Intensity weighted average fluorescence lifetimes, where multiexponential fluorescence decay is observed. [c] Interpreted as the fluorescence lifetime component of dye bound to BSA at quenching sites.

Two-fold sulfonation of the chromophore (**3**) resulted in mono-exponential fluorescence decay reveals a homogeneous solvation of the chromophore. However, a large simultaneous drop in both FLT (12.5 ns) and QY (0.28) (Table 1) show that the sulfonation indeed accelerates non-radiative deactivation. The negative impact on FLY and QY from core sulfonation is confirmed by the mono sulfonated derivative **2**, which furthermore exerts a bi-exponential decay, indicating remaining problems with aggregation of this overall neutral species.

The mono-exponential decays of **4** and **5** both show comparable FLTs above 18 ns. Along with the measured QYs (Table 1), these results indicate that the dyes are well-solvated in water as a result of the charged side chains. Remarkably, both the FLTs and QYs of these dyes are comparable to Pr_2DAOTA^+ in MeCN solution.[39]

The fluorescence decay of **6** features a small secondary component in pure water. We speculate that the charge complementarity of the two positive and two negative groups in each end of the molecule may lead to head-to-tail aggregates. The lower FLT compared to **1** must, as discussed for **2** and **3**, be attributed to the introduction of sulfonic acids groups on the chromophore core.

Solvation of dyes in buffers and protein solutions

To draw parallels to biological systems, time-resolved fluorescence of the dyes in phosphate buffered saline (PBS) was also investigated (Table 2). The obtained decays were mostly similar to the ones observed in pure water. For **3,** a biexponential decay was observed. The increased salt concentration of the solution could lower the solvation of the dye, thus inducing aggregation to some extent.[60] Inversely, a mono-exponential decay for **6** in PBS could be due to the breaking up of the proposed head-to-tail aggregates due to the additional ionic strength stabilizing the solvation of the highly charged dye. It should be noted, however, that for either dye these are relatively small effects.

The fluorescence lifetime measurements were repeated with the addition of 600 µM BSA to introduce sites for non-specific binding, relatable to biologically relevant media.[61] For all dyes an additional short-lived component was observed, leading to an overall decrease in the average FLT. The short-lived component is more prevalent for the dyes that already display compromised solvation in PBS. We tentatively assign the short lived component to dye bound to BSA at a quenching site. Especially the core sulfonated anionic dye, **3**, shows to be severely compromised at high protein concentrations. This observation is noteworthy since sulfonation and overall negative charge is the preferred modification for many commercial fluorescence dyes.

The well-solvated and bright chromophores, **4** and **5** are only slightly affected by BSA. The population of freely dissolved chromophores in these cases does not seem to be affected by the presence of BSA at retaining the long FLT of 18 ns, while a small fraction of the molecules bound to BSA display a 6-8 ns lifetime. The interaction between dye molecules and BSA must therefore be static on the nanosecond timescale. Any significant presence of one or more "dark" interactions with the protein can be ruled out based on the relative fluorescence intensities, which show a reduction of 6-10 % upon addition of BSA (Figures S10-S11).

Intrinsic water quenching

Aside from solubility and solvation, fluorescence of organic chromophores in water is further complicated by a quenching effect intrinsic to the solvent. This has been illustrated several times by enhanced fluorescence intensity and FLT in D_2O.[62-65] The exact mechanism by which this

quenching occurs and what parameters affect it is still to be fully understood and it is thus difficult to predict the extent of the effect.

Measuring the FLT in D_2O for the dyes **1**-**6** (Table 3) showed a significant increase compared to H_2O. A 20 % enhancement is seen for **4** and **5** already displaying long FLTs in pure water. This effectively surpasses its parent's performance in MeCN and brings the fluorophore on par with Pr_2DAOTA^+ in DCM[39], in which a similar solvent quenching effect is not expected to take place. A 30 % enhancement is seen in the remaining cases. Where bi- exponential decays are observed, both fluorescence decay components see an increase, suggesting that even dye aggregates are affected by the quenching effect of water.

Table 3. Fluorescence lifetimes of **1**-**6** (Chart 1) in deuterium oxide and the relative increase compared to water (Table 2).

	τ_{f1} [ns]	τ_{f2} [ns] [a]	τ_{avg} [ns] [b]	$\tau_{(D2O)}/\tau_{(H2O)}$
1	19.3	27.6 (22 %)	21.1	1.27[c]
2	16.8	23.6 (32 %)	19.0	1.28[c]
3	16.6	-	-	1.33
4	21.9	-	-	1.20
5	22.1	-	-	1.19
6	19.2	-	-	1.28[c]

[a] Secondary fluorescence lifetime components and their weighted intensities in parenthesis. [b] Amplitude weighted average fluorescence lifetimes, where multiexponential fluorescence decay is observed. [c] Value calculated based on the intensity weighted average fluorescence lifetime for bi-exponential decays.

Rates of the excited state processes

With the steady state and time-resolved fluorescence results in hand we can now look at how the structural differences of the dyes affect the associated excited state deactivation processes. Calculating the rate constants (Table 4) from the measured FLTs and QYs reveals that **4** and **5** featuring the hydrophilic side chains have a significantly higher radiative rate k_f than the remaining derivatives. This effect we assign to the electrostatic impact of the positively charged ammonium group on the nitrogen donor groups in the $DAOTA^+$ chromophore, which also did result in a blueshift and narrowing of the absorption and emission bands.

Most importantly, **4** and **5** display very low rates of non-radiative deactivation k_{nr} (Table 4), showing that this design is ideal for solubilizing $DAOTA^+$ in water. This becomes even more clear when considering that almost 40 % of the non-radiative deactivation observed for these dyes in water seems to be solvent specific quenching, as can be seen by comparing the rates in water and D_2O (Table 4). Interestingly, it seems that the aromatic sulfonates attached directly to the chromophore core opens up additional paths of non-radiative deactivation increasing k_{nr} by a factor of two. This is most clearly seen by comparison between the derivatives well solvated in D_2O where effects of aggregation and specific water quenching are not contributing. Here the core sulfonated compounds **3** and **6** display k_{nr} twice that of **4** and **5.**

Table 4. Radiative and non-radiative rate constants for the depopulation of the excited state of **1**-**6** in water and deuterium oxide.

	k_f [10^7 s^{-1}]	$k_{nr\ (H2O)}$ [10^7 s^{-1}]	$k_{nr\ (D2O)}$ [a] [10^7 s^{-1}]	Δk_{nr} [b] [10^7 s^{-1}]
Pr_2DAOTA^+ [c, d]	2.6	2.1	-	-
1[e]	2.0	4.5	3.1	1.4
2[e]	2.0	5.4	4.0	1.5
3	2.2	5.8	3.8	2.0
4	3.1	2.4	1.5	0.9
5	3.0	2.4	1.5	0.9
6[e]	2.5	4.4	2.7	1.6

[a] The rate constant of fluorescence is assumed to be the same in water and deuterium oxide. [b] Effectively the quenching contribution of water, kQ·[Q]. [c] In acetonitrile. [d] Data from Bogh et al. (2017).[39] [e] Rate constants calculated from dominant component of biexponential decay fits.

Conclusions

Six new water-soluble $DAOTA^+$-derivatives were obtained through combinations of three different strategies for modifying the chromophore. Exchanging the lipophilic anion for chloride (**1**) lead to a substantial gain in water solubility, but solvation and aggregation of the cationic chromophore remain unaltered. While twofold direct sulfonation of the $DAOTA^+$ chromophore (**3**) does enhance solvation in pure water, aggregation and non-specific binding are still a concern in biologically relevant environments. Despite further effort to modify $DAOTA^+$ in this regard (**6**),

core modifications remain problematic as the introduction of additional non-radiative deactivation pathways compromises fluorescence lifetime and quantum yield. Excellent photophysical properties in water resulted from introducing charged side chains in derivatives **4** and **5**. This design strategy resulted in dyes with long FLT of 18 ns and high quantum yields of 56 %, to our knowledge, unmatched by any other water-soluble small molecule fluorophores emitting beyond 550 nm. We managed to utilize the FLT response as a tool to investigate how different solvation strategies influence molecular events and interactions. These results help in finding the optimal design for a bioconjugable and water-soluble FLT probe.

In first instance these results suggest that charged and zwiterionic side chains most likely also are a preferable design strategy for organic fluorophores in general over traditional core sulfonation.

The potential usefulness of this strategy extends beyond the field of dyestuff. Tuning solvation through different functionalizations is useful in several fields, e.g. in the science of nanostructures, where controlled self-assembly in various solvents is of interest. Long FLT probes hold potential as tools for investigating such solvation effects. We see the $DAOTA^+$ chromophore as a good candidate for further investigation of such properties, in particular due to the sensitivity and resolution of time-resolved fluorescence spectroscopy as demonstrated. These dyes should also be considered in the investigation of fluorescence quenching effects, since time-resolved measurements are much more sensitive and convenient than corresponding intensity-based experiments. Further, they provide detailed information on effects causing changes in fluorescence response. Through combinations of these approaches, valuable information on the time scales of the investigated events can be had, allowing for discrimination between static and dynamic molecular events.

Conflicts of interest

The authors declare the following competing financial interests: Bo W. Laursen is associated with the company KU-dyes, which produces and sells fluorescent dyes (including triangulenium dyes).

Acknowledgements

The work was supported by the Danish Council of Independent Research (DFF-6111-00483).

References

1. G. L. Perlovich, A. O. Surov and A. Bauer-Brandl, *J Pharm Biomed Anal*, 2007, **45**, 679-687.

2. K. Ariga, M. Nishikawa, T. Mori, J. Takeya, L. K. Shrestha and J. P. Hill, *Sci Technol Adv Mater*, 2019, **20**, 51-95.

3. E. Oliveira, E. Bertolo, C. Nunez, V. Pilla, H. M. Santos, J. Fernandez-Lodeiro, A. Fernandez-Lodeiro, J. Djafari, J. L. Capelo and C. Lodeiro, *Chemistryopen*, 2018, **7**, 9-52.

4. A. N. Butkevich, V. N. Belov, K. Kolmakov, V. V. Sokolov, H. Shojaei, S. C. Sidenstein, D. Kamin, J. Matthias, R. Vlijm, J. Engelhardt and S. W. Hell, *Chemistry*, 2017, **23**, 12114-12119.

5. X. Wang, Y. Z. Hu, A. Chen, Y. Wu, R. Aggeler, Q. Low, H. C. Kang and K. R. Gee, *Chem Commun (Camb)*, 2016, **52**, 4022-4024.

6. C. A. Hunter and J. K. M. Sanders, *J Am Chem Soc*, 1990, **112**, 5525-5534.

7. D. Chandler, *Nature*, 2005, **437**, 640-647.

8. J. Li, N. Kwon, Y. Jeong, S. Lee, G. Kim and J. Yoon, *ACS Appl Mater Interfaces*, 2018, **10**, 12150-12154.

9. M. Collot, T. K. Fam, P. Ashokkumar, O. Faklaris, T. Galli, L. Danglot and A. S. Klymchenko, *J Am Chem Soc*, 2018, **140**, 5401-5411.

10. N. J. Hestand and F. C. Spano, *Acc Chem Res*, 2017, **50**, 341-350.

11. K. Tani, C. Ito, Y. Hanawa, M. Uchida, K. Otaguro, H. Horiuchi and H. Hiratsuka, *J Phys Chem B*, 2008, **112**, 836-844.

12. A. B. Descalzo, P. Ashokkumar, Z. Shen and K. Rurack, *Chemphotochem*, 2019, **4**, 120-131.

13. R. L. Halterman, J. L. Moore and W. T. Yip, *J Fluoresc*, 2011, **21**, 1467-1478.

14. L. C. Zanetti-Domingues, C. J. Tynan, D. J. Rolfe, D. T. Clarke and M. Martin-Fernandez, *Plos One*, 2013, **8**, e74200.

15. C. Sanchez-Rico, L. Voith von Voithenberg, L. Warner, D. C. Lamb and M. Sattler, *Chemistry*, 2017, **23**, 14267-14277.

16. L. D. Hughes, R. J. Rawle and S. G. Boxer, *Plos One*, 2014, **9**, e87649.

17. Y. S. Zeng, R. C. Gao, T. W. Wu, C. Cho and K. T. Tan, *Bioconjug Chem*, 2016, **27**, 1872-1879.

18. N. Panchuk-Voloshina, R. P. Haugland, J. Bishop-Stewart, M. K. Bhalgat, P. J. Millard, F. Mao, W. Y. Leung and R. P. Haugland, *J Histochem Cytochem*, 1999, **47**, 1179-1188.

19. F. Mao, W. Y. Leung and R. P. Haugland, 1999, WO9915517.

20. W. Lin and T. Chen, *Anal Biochem*, 2013, **443**, 252-260.

21. S. Daddi Oubekka, R. Briandet, M. P. Fontaine-Aupart and K. Steenkeste, *Antimicrob Agents Chemother*, 2012, **56**, 3349-3358.

22. K. Suhling, J. Levitt and P. H. Chung, *Methods Mol Biol*, 2014, **1076**, 503-519.

23. K. Kolmakov, V. N. Belov, J. Bierwagen, C. Ringemann, V. Muller, C. Eggeling and S. W. Hell, *Chemistry*, 2010, **16**, 158-166.

24. K. Kolmakov, C. A. Wurm, R. Hennig, E. Rapp, S. Jakobs, V. N. Belov and S. W. Hell, *Chemistry*, 2012, **18**, 12986-12998.

25. H. J. Wories, J. H. Koek, G. Lodder, J. Lugtenburg, R. Fokkens, O. Driessen and G. R. Mohn, *Recl Trav Chim Pay B*, 1985, **104**, 288-291.

26. L. Li, J. Han, B. Nguyen and K. Burgess, *J Org Chem*, 2008, **73**, 1963-1970.

27. S. L. Niu, G. Ulrich, R. Ziessel, A. Kiss, P. Y. Renard and A. Romieu, *Org Lett*, 2009, **11**, 2049-2052.

28. T. Bura and R. Ziessel, *Org Lett*, 2011, **13**, 3072-3075.

29. S. L. Niu, C. Massif, G. Ulrich, P. Y. Renard, A. Romieu and R. Ziessel, *Chemistry*, 2012, **18**, 7229-7242.

30. A. Romieu, D. Tavernier-Lohr, S. Pellet-Rostaing, M. Lemaire and P.-Y. Renard, *Tetrahedron Letters*, 2010, **51**, 3304-3308.

31. A. Romieu, T. Bruckdorfer, G. Clave, V. Grandclaude, C. Massif and P. Y. Renard, *Org Biomol Chem*, 2011, **9**, 5337-5342.

32. C. Massif, S. Dautrey, A. Haefele, R. Ziessel, P. Y. Renard and A. Romieu, *Org Biomol Chem*, 2012, **10**, 4330-4336.

33. K. Kolmakov, V. N. Belov, C. A. Wurm, B. Harke, M. Leutenegger, C. Eggeling and S. W. Hell, *European Journal of Organic Chemistry*, 2010, **2010**, 3593-3610.

34. R. M. Rich, D. L. Stankowska, B. P. Maliwal, T. J. Sorensen, B. W. Laursen, R. R. Krishnamoorthy, Z. Gryczynski, J. Borejdo, I. Gryczynski and R. Fudala, *Anal Bioanal Chem*, 2013, **405**, 2065-2075.

35. B. P. Maliwal, R. Fudala, S. Raut, R. Kokate, T. J. Sorensen, B. W. Laursen, Z. Gryczynski and I. Gryczynski, *Plos One*, 2013, **8**, e63043.

36. A. Shivalingam, M. A. Izquierdo, A. L. Marois, A. Vysniauskas, K. Suhling, M. K. Kuimova and R. Vilar, *Nat Commun*, 2015, **6**, 8178.

37. T. J. Sørensen, E. Thyrhaug, M. Szabelski, R. Luchowski, I. Gryczynski, Z. Gryczynski and B. W. Laursen, *Methods Appl Fluores*, 2013, **1**, 025001.

38. S. A. Bogh, I. Bora, M. Rosenberg, E. Thyrhaug, B. W. Laursen and T. J. Sorensen, *Methods Appl Fluoresc*, 2015, **3**, 045001.

39. S. A. Bogh, M. Simmermacher, M. Westberg, M. Bregnhoj, M. Rosenberg, L. De Vico, M. Veiga, B. W. Laursen, P. R. Ogilby, S. P. A. Sauer and T. J. Sorensen, *Acs Omega*, 2017, **2**, 193-203.

40. T. J. Sørensen, M. Rosenberg, C. G. Frankær and B. W. Laursen, *Advanced Materials Technologies*, 2018, **4**, 1800561.

41. I. Dalfen, R. I. Dmitriev, G. Holst, I. Klimant and S. M. Borisov, *Anal Chem*, 2019, **91**, 808-816.

42. I. Bora, S. A. Bogh, M. Rosenberg, M. Santella, T. J. Sorensen and B. W. Laursen, *Org Biomol Chem*, 2016, **14**, 1091-1101.

43. E. Thyrhaug, T. J. Sorensen, I. Gryczynski, Z. Gryczynski and B. W. Laursen, *J Phys Chem A*, 2013, **117**, 2160-2168.

44. C. Herse, D. Bas, F. C. Krebs, T. Burgi, J. Weber, T. Wesolowski, B. W. Laursen and J. Lacour, *Angew Chem Int Ed Engl*, 2003, **42**, 3162-3166.

45. M. Rosenberg, K. R. Rostgaard, Z. Liao, A. O. Madsen, K. L. Martinez, T. Vosch and B. W. Laursen, *Chem Sci*, 2018, **9**, 3122-3130.

46. M. Rosenberg, M. Santella, S. A. Bogh, A. V. Munoz, H. O. B. Andersen, O. Hammerich, I. Bora, K. Lincke and B. W. Laursen, *J Org Chem*, 2019, **84**, 2556-2567.

47. O. Kel, P. Sherin, N. Mehanna, B. Laleu, J. Lacour and E. Vauthey, *Photochem Photobiol Sci*, 2012, **11**, 623-631.

48. J. Guin, C. Besnard and J. Lacour, *Org Lett*, 2010, **12**, 1748-1751.

49. Y. K. Yang and J. Tae, *Org Lett*, 2006, **8**, 5721-5723.

50. A. Joshi-Pangu, F. Levesque, H. G. Roth, S. F. Oliver, L. C. Campeau, D. Nicewicz and D. A. DiRocco, *J Org Chem*, 2016, **81**, 7244-7249.

51. J. B. Grimm, A. K. Muthusamy, Y. Liang, T. A. Brown, W. C. Lemon, R. Patel, R. Lu, J. J. Macklin, P. J. Keller, N. Ji and L. D. Lavis, *Nat Methods*, 2017, **14**, 987-994.

52. M. Beija, C. A. Afonso and J. M. Martinho, *Chem Soc Rev*, 2009, **38**, 2410-2433.

53. B. W. Laursen and F. C. Krebs, *Chem-Eur J*, 2001, **7**, 1773-1783.

54. I. H. Delgado, S. Pascal, C. Besnard, S. Voci, L. Bouffier, N. Sojic and J. Lacour, *Chemistry*, 2018, **24**, 10186-10195.

55. I. H. Delgado, S. Pascal, A. Wallabregue, R. Duwald, C. Besnard, L. Guenee, C. Nancoz, E. Vauthey, R. C. Tovar, J. L. Lunkley, G. Muller and J. Lacour, *Chem Sci*, 2016, **7**, 4685-4693.

56. X.-M. Hu, Q. Chen, Z.-Y. Sui, Z.-Q. Zhao, N. Bovet, B. W. Laursen and B.-H. Han, *Rsc Adv*, 2015, **5**, 90135-90143.

57. R. Duwald, S. Pascal, J. Bosson, S. Grass, C. Besnard, T. Burgi and J. Lacour, *Chemistry*, 2017, **23**, 13596-13601.

58. P. Shieh, V. T. Dien, B. J. Beahm, J. M. Castellano, T. Wyss-Coray and C. R. Bertozzi, *J Am Chem Soc*, 2015, **137**, 7145-7151.

59. E. Thyrhaug, T. J. Sorensen, I. Gryczynski, Z. Gryczynski and B. W. Laursen, *J Phys Chem A*, 2013, **117**, 2160-2168.

60. A. K. Chibisov, H. Görner and T. D. Slavnova, *Chem Phys Lett*, 2004, **390**, 240-245.

61. G. L. Trainor, *Expert Opin Drug Discov*, 2007, **2**, 51-64.

62. P. Taborsky, J. Kucera, J. Jurica and O. Pes, *J Chromatogr B Analyt Technol Biomed Life Sci*, 2018, **1092**, 7-14.

63. K. Klehs, C. Spahn, U. Endesfelder, S. F. Lee, A. Furstenberg and M. Heilemann, *Chemphyschem*, 2014, **15**, 637-641.

64. J. Olmsted, 3rd and D. R. Kearns, *Biochemistry*, 1977, **16**, 3647-3654.

65. J. Kucera, P. Lubal, S. Lis and P. Taborsky, *Talanta*, 2018, **184**, 364-368.